Supplementary Materials for

Stochastic tunneling across fitness valleys can give rise to a logarithmic long-term fitness trajectory

Yipei Guo, Marija Vucelja, Ariel Amir*

*Corresponding author. Email: arielamir@seas.harvard.edu

This PDF file includes:

Supplementary materials

Section SA. Choice of null model for the combined effect of multiple independent mutations

We have assumed the additive null model for epistasis in our model. Another commonly used multiplicative model states that the growth rate F_n of a cell with n independent mutations is given by $F_n = F_0(1+s_1)(1+s_2)...(1+s_n)$, implying that $\log(F_n) = \log(F_0) + \sum_i^n \log(1+s_i)$. This corresponds to our original fitness function (main text Eqn. 1) if we replace F with $\log(F)$. The fixation probability of a mutation at site i will now be proportional to $\frac{\Delta F}{F} = \Delta \log(F) \propto |h_i|$ instead of $\frac{|h_i|}{F}$ in the original additive model.

When the dynamics is governed by hopping between metastable states, the logarithmic trajectory is driven by the structure of the landscape rather than the specific details of the transition rates between states. The multiplicative null model for microscopic epistasis would therefore give a logarithmic trajectory for $\log(F) \sim a \log(t)$, which implies that $F \sim t^a$. If a is small, one would also get an increase in fitness that resembles a logarithmic function.

Section SB. Range of validity for population size N

In our model, we make the following assumptions:

1. Within the hill-climbing regime, $p_f(s) = \max(s, 0)$. This is true if

$$N \gg 1/s \qquad \text{(S1)}$$

For this to always hold at all times during the simulation, this condition must apply for $s = s_{b,min}$, where $s_{b,min}$ is the smallest fitness effect among all beneficial mutations. However, since the average trajectory is dominated by the typical behaviour, this assumption is reasonable as long as the Eqn.S1 holds for the average fitness effect of fixed mutations $\langle s_{fix} \rangle = \frac{\int s^2 P(s) ds}{\int s P(s)}$, where $P(s)$ is the distribution of fitness effects.

2. No clonal interference (SSWM limit). This means that the time taken for a beneficial mutation with fitness effect s to fix $\tau_{fix} = \frac{\log(Ns)}{s}$ is much shorter than the average time for the next successful mutation to emerge $\tau_{emerge} = \frac{1}{N\mu\langle p_f(s)\rangle}$, where the average $\langle\rangle$ is taken over all L sites. Together with the previous assumption that $p_f(s) = s$ for beneficial mutations, the condition for this to always be true becomes: $N\mu_b \frac{\langle s_b\rangle}{s_{b,min}}\log(Ns_{b,min}) \ll 1$, where μ_b is the beneficial mutation rate, $\langle s_b\rangle$ is the average beneficial fitness effect and as before, $s_{b,min}$ is the weakest available beneficial mutation.

However, the probability of $s_{b,min}$ emerging is low, and hence an adequate condition that takes into account the distribution $P(s)$ of mutations s that try to fix is:

$$\int N\mu_b \frac{\langle s_b\rangle}{s}\log(Ns)P(s)ds \ll 1 \tag{S2}$$

3. At a metastable state, the probability of a stochastic tunneling event outweighs that of a deleterious mutation fixation event, even when there is only one possible stochastic tunneling path out for the state. Denoting the average probability of a first mutant becoming a successful double mutant (given that there exists a stochastic tunneling path through that first mutant) as $p_{d,av}$ (Eqn.4), this assumption requires that:

$$p_{d,av} \gg \sum_{i=1}^{L} p_f(s_1^{(i)}) = \frac{L}{N}\int_{-\infty}^{s_{1,max}} e^{-N|s_1|}P(s_1)ds_1 \tag{S3}$$

where $P(s_1)$ is the distribution of first mutation effects from a metastable state and $s_{1,max}$ is the upper bound of this distribution.

Given the parameters $L = 200$, $\rho = 0.05$, $\beta = 0.9$, $\Delta = 0.05$ (which together give the distribution of fitness effects) used in our main simulations (Fig. 3), we find numerically (by sampling 100 states on 10 quenched landscapes) that $\langle s_{fix}\rangle \sim 10^{-2}$. Our first condition (Eqn.S1) therefore gives $N \gg 10^2$.

Similarly, we find numerically that for $\mu_b = \mu = 10^{-8}$, our second condition (Eqn.S2) gives $N \ll 10^{6.5}$. In our case, since the states in our simulations are close to fitness peaks, the fraction of beneficial mutation sites out of L is at most about 0.1. Therefore $\mu_b = 0.1 \cdot \mu = 10^{-9}$ which gives the condition that $N \ll 10^{7.5}$.

By sampling metastable states, we find that $|s_{1,max}| \sim 10^{-5}$, and the upper bound to $\frac{\sqrt{\langle s_{eff} \rangle}}{|s_1|}$ is $\sim 10^2$, which gives $\frac{\sqrt{\mu \langle s_{eff} \rangle}}{|s_1|} \lesssim 10^{-2}$. This implies that we are almost always in the deep valley regime where $p_d = \frac{\mu \langle s_{eff} \rangle}{|s_1|}$ (Eqn.4), and with our parameters, for the case where there is just one possible stochastic tunneling path, $p_{d,av} = \frac{\mu}{L} \langle \left(\frac{s_{eff}}{|s_1|} \right) \rangle \sim 10^{-9}$. Solving the integral in Eqn.S3 numerically, we find that this third condition gives $N \gg 10^5$. However, in practice, even if nearly-neutral deleterious mutations occasionally fix, the same back mutation will occur with high probability as long as there are not too many of these weak deleterious mutations available. In fact, we find numerically (by specifying a population size N and allowing deleterious mutations with $|s_1| < 1/N$ to fix) that even for population size of 10^4, we still observe a similar logarithmic trajectory (data not shown).

It is also useful to note that decreasing μ while keeping the other parameters (and hence fitness effect distributions) the same will increase the upper bound of N (that comes from clonal interference) while keeping the lower bound relatively constant, thereby increasing the range of N that falls within our regime of interest.

Section SC. Structural features of fitness landscapes

Since the dynamics of fitness is governed by the structure of the fitness landscape, we investigated how these properties vary with L by randomly sampling fitness peaks of a quenched landscape. The random samples of fitness peaks were obtained by randomly specifying a state and randomly flipping beneficial sites (i.e. sites that provide an increase in fitness when mutated are chosen with equal probability) until there are no longer any beneficial mutations left.

By assuming that the average fitness effect of mutations is independent of L (which is consistent with the scaling $\sigma_h \sim O(1)$ and $\sigma_J \sim 1/\sqrt{\rho L}$), the average values of fitness peaks within our model increases linearly with L (Fig.S1a).

Since we have only included pairwise interactions, the landscape is highly correlated. This is in contrast to the uncorrelated House of Cards (HoC) landscape where fitness values of every state is drawn independently from the same distribution.

To understand the correlation structure of the landscape, we consider without loss of generality the state $\vec{x} = [-1, -1, \ldots -1]$ with fitness $F_x = -\sum_i h_i + \sum_{i<j} J_{ij}$. A state $\vec{y}$ with the first k spins flipped will then have fitness $F_y = F_x + 2\sum_{i=1}^{k} h_i - 2\sum_{i=1}^{k} \sum_{j=k+1}^{L} J_{ij}$, where k is also the hamming distance between the two states. To calculate the correlation $C(F_x, F_y)$ between two states a distance k apart, we will need to take average over all states with k spin flips, but this is equivalent to taking an average over the variables h and J, which we denote using angular brackets $\langle \rangle$. Since $\langle h_i h_j \rangle = \delta_{ij} \sigma_h^2$ and $\langle J_{ij} J_{kl} \rangle = \delta_{ik} \delta_{jl} \sigma_J^2$ for $|J_{ij}| > 0$, we have

$$
\begin{aligned}
C(F_x, F_y) &= \frac{\langle F_x F_y \rangle - \langle F_x \rangle \langle F_y \rangle}{\sigma_F^2} \\
&= \left(\langle F_x^2 \rangle + 2 \langle F_x \sum_{i=1}^{k} h_i \rangle - 2 \langle F_x \sum_{i=1}^{k} \sum_{j=1+k}^{L} J_{ij} \rangle \right) / \sigma_F^2 \\
&= 1 - 2k \frac{\sigma_h^2}{\sigma_F^2} - 2k(L-k)\rho \frac{\sigma_J^2}{\sigma_F^2} \\
&= 1 - 2\frac{k}{L} \frac{\tilde{\sigma}_h^2}{\sigma_F^2} - 4\frac{k}{L} \left(1 - \frac{k}{L} \right) \frac{\tilde{\sigma}_J^2}{\sigma_F^2}
\end{aligned}
\tag{S4}
$$

where $\tilde{\sigma}_h^2 = L\sigma_h^2$, $\tilde{\sigma}_J^2 = \frac{\rho L^2}{2}\sigma_J^2$, and the variance in fitness $\sigma_F^2 = \tilde{\sigma}_h^2 + \tilde{\sigma}_J^2$. With $\sigma_h = (1-\beta)\Delta$ and $\sigma_J = \beta\Delta/\sqrt{\rho L}$, both $\frac{\tilde{\sigma}_h^2}{\sigma_F^2} = \frac{2(1-\beta)^2}{2(1-\beta)^2 + \beta^2}$ and $\frac{\tilde{\sigma}_J^2}{\sigma_F^2} = 1 - \frac{\tilde{\sigma}_h^2}{\sigma_F^2}$ are independent of k and L. The correlation between two states is therefore only a function of k/L, and the form of $C(F_x, F_y)$ signifies the presence of long range correlations. This expression for $C(F_x, F_y)$ was also verified numerically by calculating the correlation between fitness values of states as a function of their hamming distance (Fig.S1b).

Similarly, both the average number of steps N_{steps} it takes for a randomly drawn state to reach a fitness peak and the average hamming distance d between connected metastable states (two MS are connected if one of them can be reached from the other via a beneficial double mutation possibly followed by beneficial single mutations) also scale linearly with L (Fig.S1c,d). In contrast, for a HoC landscape, $N_{steps} \sim \log(L)$.

C..1 Stability of metastable states to double mutations

Since within our model a system can only escape from metastable states via beneficial double mutants (which is only possible if the fitness peak is unstable to double mutations), we investigated the stability of 100 randomly sampled local fitness peaks in any specified landscape within our model, and found that when interactions are sparse, almost all these states are metastable states that are unstable to double mutations (Fig. S1e). This is in contrast to having a much larger density of interactions such as $\rho = 0.5$ where there is a significant fraction of local fitness peaks that are stable to all possible double mutations (Fig. S1e). For the standard fully-connected SK model ($\rho = 1$), $P_{unstable}$ plateau off at ~ 0.7 (Data not shown).

C..2 Number of escape paths out of a metastable state

In addition to $P_{unstable}$ which indicates the presence of at least one escape path out of a fitness peak, the number of such double mutant escape states n_p will also affect adaptation dynamics on the landscape. By again averaging over many metastable states, we find that n_p decreases sharply with ρ (Fig. S1f).
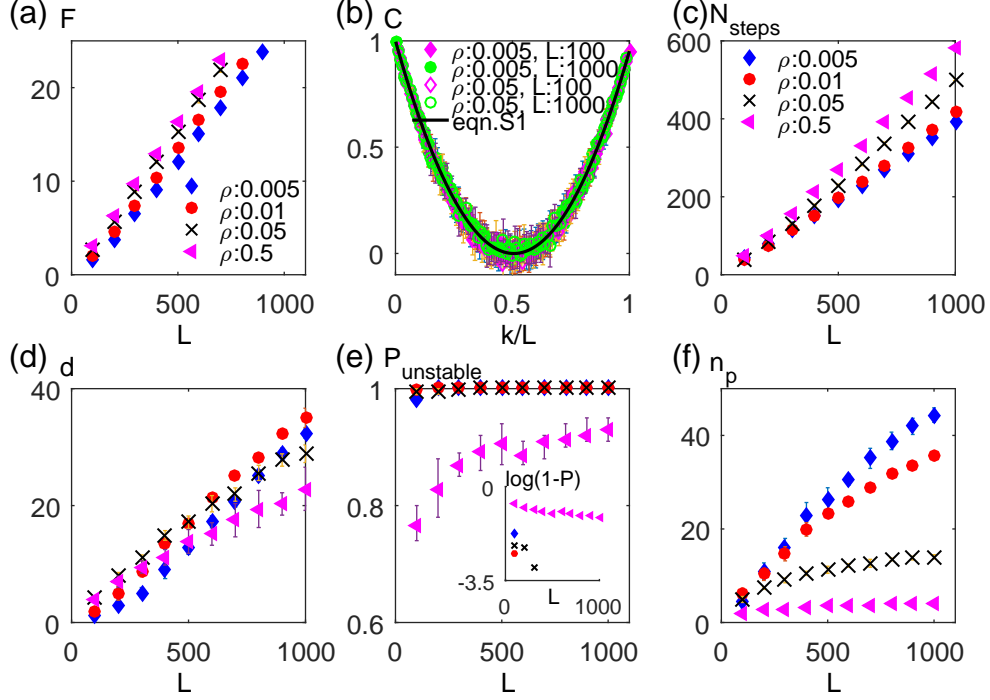
Fig. S1. Properties of fitness landscape as a function of L. In (a) and (c)-(f), data is shown for $\rho = 0.005$ (blue diamonds), $\rho = 0.01$ (red circles), $\rho = 0.05$ (black crosses), $\rho = 0.5$ (purple triangles). (a) Average fitness of peaks increases linearly with L. (b) Correlation between two states is only a function of k/L, where k is the hamming distance between the two states. Data is shown for $L = 100$ (purple diamonds) and $L = 1000$ (green circles), with $\rho = 0.005$ (filled markers) and $\rho = 0.05$ (unfilled markers). All data sets collapse and fit well to the analytical expression (black line, Eqn.S4). Both (c) the average number of steps to a fitness peak N_{steps} and (d) the average hamming distance between connected metastable states scale linearly with L. (e) The fraction of metastable states that are unstable to two mutations ($P_{unstable}$) plateau to 1 as L increases for small values of ρ but seems to stabilize at a lower value for much larger values of ρ. The inset plots $log_{10}(1 - P_{unstable})$ as a function of L. Data points are not plotted when all fitness peaks sampled are metastable states. (f) The average number of escape paths from a metastable state increases with L, with the rate of increase higher for smaller ρ. All crosses represent averages taken over 100 randomly chosen states on a quenched landscape, and error bars represent standard deviations over 10 different quenched landscapes. [other parameters: $\beta = 0.9, \Delta = 0.05, F_{offset} = 0$]

C..3 Including weak dense pairwise interactions

We also consider the more general scenario where all sites interact weakly with one another, in addition to having strong, sparse interactions:

$$F = \sum_{i=1} h_i \alpha_i + \sum_{i<j} J_{ij}^S \alpha_i \alpha_j + \sum_{i<j} J_{ij}^F \alpha_i \alpha_j + F_{offset} \tag{S5}$$

where J^S is the sparse J matrix in our main model (Eqn.1), while J^F is now a fully-filled interaction matrix with elements $J^F_{ij} \sim \mathcal{N}(0, \sigma^2_{JF})$. By having $\sigma_h = (1 - \beta_1 - \beta_2)\Delta$, $\sigma_{JS} = \beta_1 \Delta / \sqrt{\rho L}$, and $\sigma_{JF} = \beta_2 \Delta / L$, the relative contributions of the three terms can be tuned using β_1 and β_2.

We find that having this additional J^F term with a small β_2 does not seem to change the values of $P_{unstable}$ and n_p (compare Fig.S2 with Fig.S1f,e). This suggests that our results for the long-term dynamics of average fitness trajectories hold as long as the sparse interactions between sites are strong.
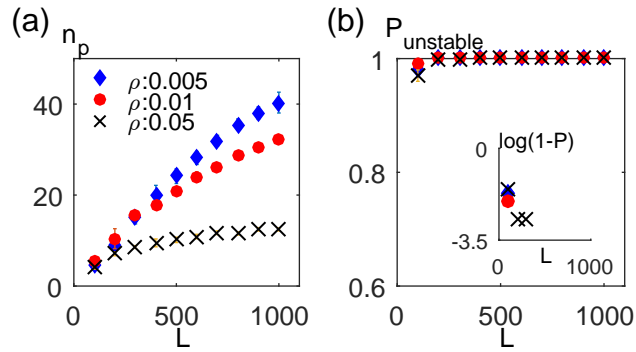

Fig. S2. Properties of fitness peaks as a function of L when additional weak interactions between all sites are included. Both the number of double mutant escape states out of a metastable state n_p(a) and the probability that a randomly chosen fitness peak is a metastable state $P_{unstable}$(b) remains approximately the same as in Fig.S1f,e for $\rho = 0.005$ (blue diamonds), $\rho = 0.01$ (red circles), and $\rho = 0.05$ (black crosses). [other parameters: $\beta_1 = 0.8, \beta_2 = 0.1, \Delta = 0.05, F_{offset} = 0$]

C..4   Properties of metastable states are correlated with fitness

Since the dynamics seems to be governed by the structure of the landscape, in particular the property that the number of escape states decreases exponentially with fitness, it is useful to probe these features of the landscape by randomly drawing metastable states instead of only using the states stored in a Markov chain.

We find that on average, the trapping time of a metastable state increases exponentially with

fitness and is predominantly due to an approximately exponential decrease in the number of escape paths with fitness (Fig. S3). These observations for how metastable state properties vary with fitness also hold for other values of ρ (Fig. S3).
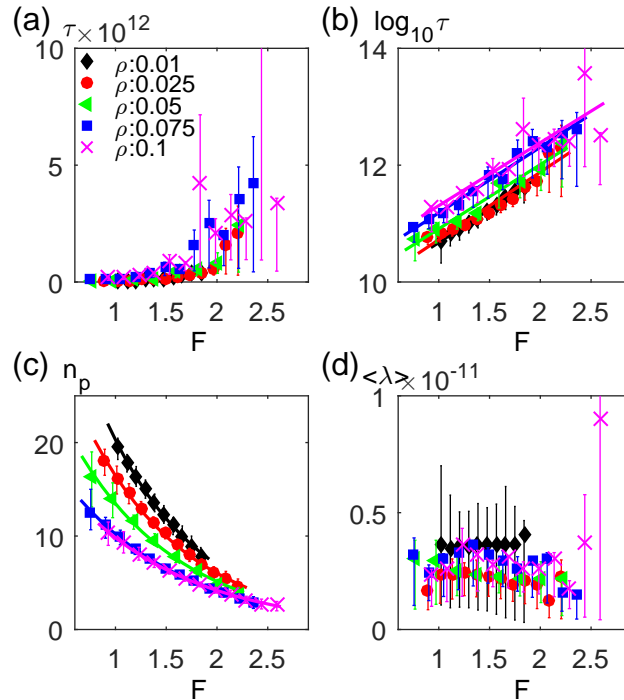

Fig. S3. Figure showing how properties of MSs vary with fitness for $\rho = 0.01$ (black diamonds, $F_{offset} = -3.4$), $\rho = 0.025$ (red circles, $F_{offset} = -3.8$), $\rho = 0.05$ (green triangles, $F_{offset} = -4.2$), $\rho = 0.075$ (blue squares, $F_{offset} = -4.4$), and $\rho = 0.1$ (purple crosses, $F_{offset} = -4.5$). Here the metastable states were obtained by starting with a random initial state and randomly flipping beneficial sites until a metastable state is reached. The dots are the averaged values among 100 sets of data, each set consisting of 500 metastable states. The error bars span the interquartile range. (a,b) Average trapping time of a metastable state increases approximately exponentially with fitness. In (b), the lines are fits to the linear function. (c) Number of escape paths (i.e. double mutant states) out of a metastable state seems to decrease exponentially with fitness. The lines are fit to the exponential function. (d) The average rate out of a metastable state to any other beneficial double mutant state is approximately the same for different fitness values. [parameters: $L = 200$, $\mu = 10^{-8}$, $\beta = 0.9$, $\Delta = 0.05$]

C..5 The number of other metastable states connected to a MS

Among the states within the Markov chain, we also find that the number of double mutant escape paths out of a metastable state is strongly correlated with the number of connecting metastable states, i.e., the number of metastable states that the system can transit to next from the current metastable state (Fig. S4). These two quantities are slightly different because two different paths can lead to the same metastable state and a path out of a metastable state can also lead to multiple metastable states. This suggests that the exponential decrease in the number of escape paths with fitness could be related to the exponential decrease in the number of local fitness maxima.
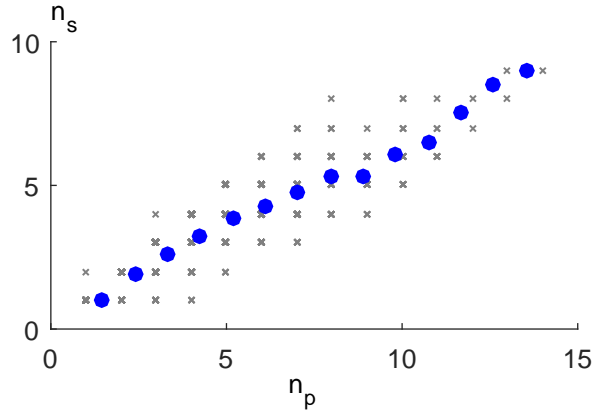

Fig. S4. The number of connecting MSs states n_s, which is the number of MSs that the system can transit to next from the current MS, correlates with the number of double mutant escape paths out of a state n_p. The grey crosses are all the individual states, while the blue dots are the averaged values. [parameters: $L = 200$, $\beta = 0.9$, $\Delta = 0.05$, $\rho = 0.05$]

Section SD. Relaxation to local fitness maximum

To investigate how relaxation to a fitness maximum varies with the degree of microscopic epistasis, we considered a strain of rank $r = L/2$, and varied the relative contributions of the field

and interaction terms by changing β from 0 to 1. For every set of quenched variables, we carried out 200 simulations starting from the same initial state, and found that the average fitness trajectories can be well fitted to the power law $F(t) = F_{max} - \frac{F_{max}-1}{(1+b_1 t)^\gamma}$, where F_{max} and b_1 are constants. The fitted parameters show that the trajectory slows down with increasing β, but is not as slow as a logarithmic trajectory (Fig.S5). The value of $\gamma = 2$ when $\beta = 0$ can also be found analytically (*27*).
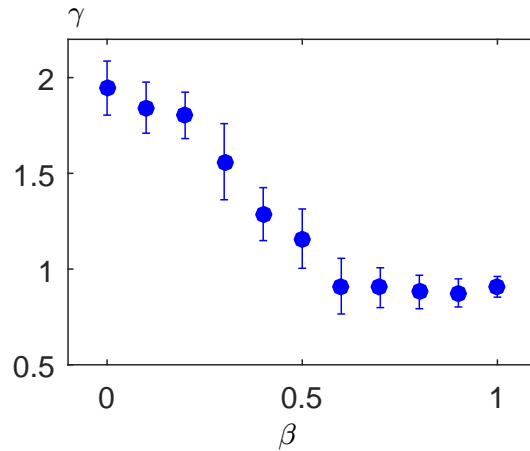
Fig. S5. Relaxation toward a single local fitness maximum slows down with increasing degree of epistasis. The fitted power law exponent of average fitness trajectory γ decreases with β. [other parameters: $L = 200$, initial rank = $L/2$, $\rho = 0.05$, $\Delta = 0.005$]

Section SE. Hopping between MSs

E..1 Random fixation probabilities

With the same tree of states as the one obtained in the example illustrated in the main text, we varied the transition matrix by drawing the fixation probability of a mutant from the uniform distribution (Fig. S6a). We found that this also gives rise to a fitness trajectory that appears to be logarithmic (Fig S6b). This suggests that the slow fitness trajectory arises predominantly from the structural property of the landscape (in particular the decrease in the number of escape

paths with increasing fitness) rather than the average rates out of the possible escape paths.
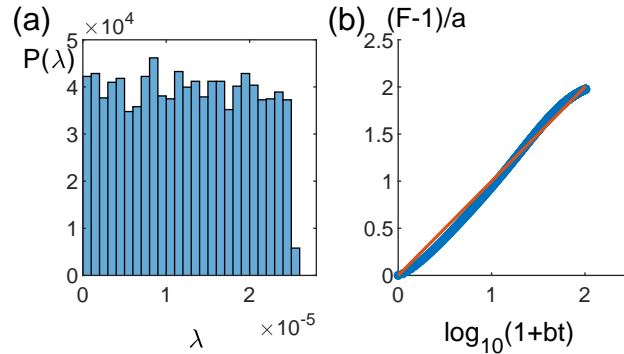

Fig. S6. Changing the distribution of fixation probabilities does not significantly change the functional form of the fitness trajectory. (a) Uniform distribution for the transition probabilities out of a metastable state. (b) Fitness trajectory is approximately logarithmic. The blue points are obtained from the Markov chain, while the red line is a fit to the logarithmic function. [parameters: $L = 200$, $\mu = 10^{-8}$, $\Delta = 0.05$, $\beta = 0.9$, $\rho = 0.05$]

E..2 Varying choice of distribution for the elements of interaction matrix

Besides drawing the non-zero elements of the interaction matrix from a Gaussian distribution, we also tried other distributions such as the two-sided exponential (Fig. S7a) and uniform (Fig. S7c), both of which also give fitness trajectories that fit well to a logarithmic function (Fig. S7b,d). Our results are therefore robust to the choice of parameter distributions.

E..3 Fitness trajectories for other values of ρ

Repeating the same analysis for different values of ρ, we find that as long as ρ is sufficiently small (so that almost all of the fitness peaks are metastable states that are unstable to two mutations (Fig.S1e) and have a significant number of escape paths (Fig.S1f)), the average fitness trajectories are approximately logarithmic (Fig.S8).
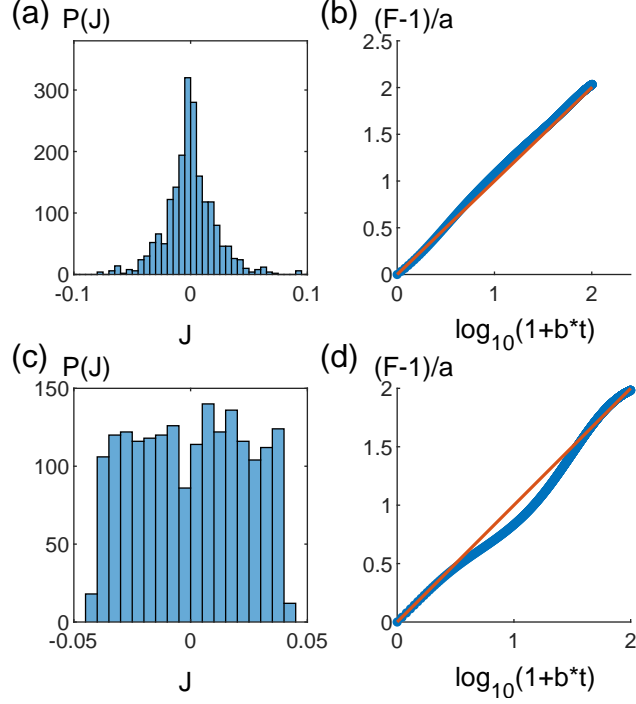
Fig. S7. Other distributions for the nonzero elements of the interaction matrix give similar form for the fitness trajectory. (a) Exponential distribution for $|J|$ gives rise to fitness trajectory in (b). (c) Uniform distribution for $|J|$ gives rise to fitness trajectory in (d) [other parameters: $L = 200$, $\mu = 10^{-8}$, $\rho = 0.05$, $\Delta = 0.05$, $\beta = 0.9$]

E..4 Aging

As the population becomes fitter, it enters states with longer and longer trapping times. Since the time taken to escape from a state increases, we expect that the correlation between the states at two different times depends not only on the time difference, but also on the initial state or time.

To test this in our model, we therefore calculate the average correlation $C(t_w, t_w + \Delta t)$ between the state $\vec{\alpha}(t_w)$ at time t_w and the state after some time $t_w + \Delta t$ given that the system starts with a specific initial state at time $t = 0$:

$$C(t_w, t_w + \Delta t) = \frac{1}{L} \left\langle \sum_{i=1}^{L} \alpha_i(t_w) \alpha_i(t_w + \Delta t) \right\rangle \tag{S6}$$
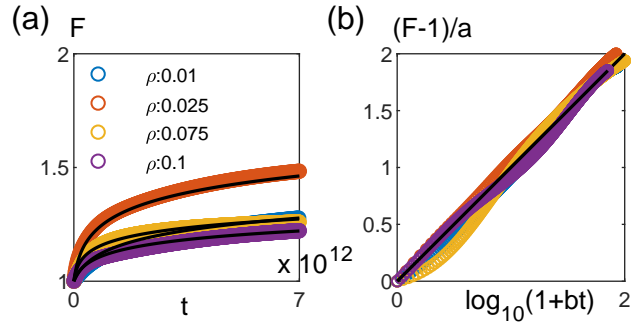
Fig. S8. Logarithmic fitness trajectories are also observed for different values of ρ. (a) Average fitness as a function of time for $\rho = 0.01$ (blue circles), $\rho = 0.025$ (red circles), $\rho = 0.075$ (yellow circles), and $\rho = 0.1$ (purple circles). Black lines are fits to the logarithmic function: $F = 1 + a\log(1 + bt)$. (b) Linear-log plot of the same data in (a). These trajectories are obtained from Markov chains constructed with the same quenched landscapes analyzed in Fig.S3. [Parameters: $L = 200$, $\mu = 10^{-8}$, $\Delta = 0.05$, $\beta = 0.9$]

where the average is taken over all possible states that the system could be in at time t_w.

As expected, we find that the decay of the correlation function is slower as t_w increases (Fig.S9).
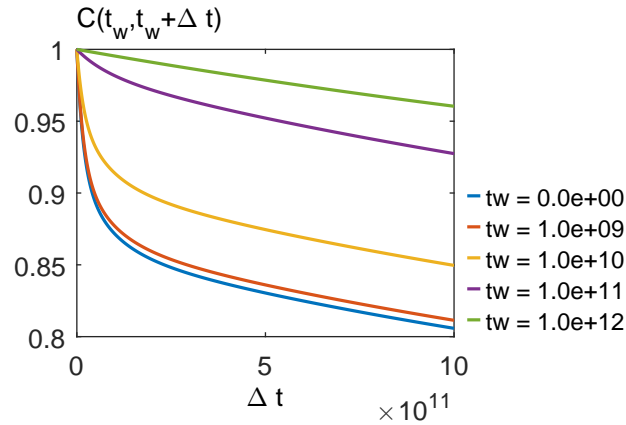

Fig. S9. The decay of the two-time correlation function depends on both the time difference Δt and the initial time of the measurement t_w, implying that the system ages. [parameters: $L = 200$, $\mu = 10^{-8}$, $\beta = 0.9$, $\Delta = 0.05$, $\rho = 0.05$]

Section SF. Batch culture

Our findings also hold for the case where cells are grown in batch culture (subject to the standard dilution protocol), after making the corresponding changes to the expression for fixation probabilities derived below.

Average fixation probabilities

Single mutants For a standard dilution protocol, we assume there are N_0 cells at the start of the day, N_f cells at the end of the day, after which a dilution of $D = \frac{N_f}{N_0}$ fold is performed. The probability $p_{ext,k}$ of k single mutants with fitness effect s at the start of a day eventually going extinct over many dilutions can be found from requiring that all daughter mutants in the next day must eventually go extinct. This can be represented by the following equation:

$$p_{ext,k} = \sum_{j=0}^{min(N_{m,k},N_0)} Hyge(j, N_{m,k}, N_f, N_0)p_{ext,j} \tag{S7}$$

where $N_{m,k} \approx kD^{1+s}$ is the number of mutants at the end of the day if we started the day with k mutants, and $Hyge(j, N_m, N_f, N_0) = \frac{\binom{N_m}{j}\binom{N_f-N_m}{N_0-j}}{\binom{N_f}{N_0}}$ is the distribution for the number of mutants drawn during the dilution process. We also demand the boundary conditions $p_{ext,0} = 1$ and $p_{ext,N_0} = 0$. Solving this set of linear equations, the fixation probability of a single mutant emerging at the start of a day can be obtained from $p_f = 1 - p_{ext,1}$. For $s = 0$, this would give $p_f = 1/N_0$.

To obtain analytical expressions for the fixation probability, we assume that $p_{ext,k} \approx p_{ext,1}^k$, which is a good approximation for the typical case where $k \ll N_0$ since in this regime the mutant cells can be considered to behave independently from one another. In the limit where $N_m, N_f, N_0 \gg 1$, $Hyge(j, N_m, N_f, N_0)$ can be approximated by the Poisson distribution with mean $\Lambda = N_0 \frac{N_m}{N_f}$. Therefore, p_f can be found approximately from the following self-consistent

equation (45):

$$p_f = 1 - \sum_{j=0} \frac{e^{-\Lambda}\Lambda^j}{j!}(1 - p_f)^j$$

$$= 1 - e^{-\Lambda p_f}$$

(S8)

For $|s|\log(D) \ll 1$, which is typically the case, this gives $p_f \approx 2\log(D)\max(s, 0)$.

However, in general the mutation can occur after some fraction of the day $\tilde{t}$ has passed. Given that a mutation has occurred, the probability that it emerged at $\tilde{t}$ is given by the probability density

$$P(\tilde{t}) = \frac{D^{\tilde{t}}\log(D)}{D - 1}$$

(S9)

For $\tilde{t} > 0$, there is a reduction in the number of mutants at the end of the first day, such that $N_m(\tilde{t}) = D^{(1+s)(1-\tilde{t})}$, and following the same argument as in Eqn.S8,

$$p_f(s, \tilde{t}) = 1 - \sum_{j=0} \frac{e^{-\tilde{\Lambda}}\tilde{\Lambda}^j}{j!}(1 - p_f(s, 0))^j$$

$$= 1 - e^{-\tilde{\Lambda}p_f(s,0)}$$

(S10)

where $\tilde{\Lambda}(\tilde{t}) = N_0 \frac{N_m(\tilde{t})}{N_f} \approx D^{-\tilde{t}}$ for $|s| \ll 1$. This gives $p_f(s, \tilde{t}) = 2\log(D)D^{-\tilde{t}}\max(s, 0)$ for $\Lambda(\tilde{t})p_f(s, 0) \ll 1$ (45).

Given that a mutation of selection coefficient s arises, its average fixation probability is then the average over all possible times within a day the mutation could have occurred:

$$\overline{p_f}(s) = \int_0^1 p_f(s, \tilde{t})P(\tilde{t})d\tilde{t}$$

$$= 2\frac{(\log(D))^2}{D - 1}\max(s, 0)$$

(S11)

Probability of successful double mutants In the large population limit, $p_f(s \leq 0) = 0$ (Eqn. S11), which implies that the population can only successfully accumulate beneficial mutations. For the population to escape a metastable state through beneficial double mutations, the first mutant (with a single deleterious mutation) must gain a second mutation before going extinct, and the effective mutant (with two mutations) must fix in the population.

Let P_{uext} be the probability that the single mutant with selection coefficient s_1 at the start of a day goes to extinction without any successful second mutation i.e. a second mutation that eventually fixes. For this to happen, there must be no successful second mutation on the first day, and all single mutants that survive to the second day must also go to extinction without gaining any successful second mutation. Adopting the same reasoning and approximations as the ones used in the derivation of p_f of a single mutant (Eqn. S8), P_{uext} can be found from the following self-consistent equation:

$$
\begin{aligned}
P_{uext} &= P_{u1} \sum_{j=0} \frac{e^{-\Lambda}\Lambda^j}{j!} P_{uext}^j \\
&= P_{u1} e^{-\Lambda(1-P_{uext})}
\end{aligned}
\tag{S12}
$$

where as before $\Lambda = D^{s_1}$, and P_{u1} is the probability that no successful second mutation occurs in the first day.

There are $N_m - 1$ single mutant division events in the first day, and there is a probability μ of a mutation occurring during each division event. For a second mutation to be successful, it will need to eventually fix and the average probability of this happening can be found following the same derivation as that for Eqn. S11:

$$
\begin{aligned}
\overline{p_f}(s_{eff}) &= \int_0^1 p_f(s_{eff}, \tilde{t}) P(\tilde{t}) d\tilde{t} \\
&= \int_0^1 \left(2\log(D) D^{-\tilde{t}} s_{eff} \right) \left(\frac{D^{(1+s_1)\tilde{t}}\log(D)(1+s_1)}{D^{1+s_1} - 1} \right) d\tilde{t} \\
&\approx 2\frac{(\log(D))^2(1+s_1)}{D^{1+s_1} - 1} s_{eff}, \text{ for } |s_1\log(D)| \ll 1
\end{aligned}
\tag{S13}
$$

where here $\tilde{t}$ is the time the double mutant emerges from the first mutant, and s_{eff} is the effective selection coefficient of the double mutant. However, since there are L possible sites that the second mutation can occur, the average fixation probability of a double mutant arising from the single mutant is given by the $\langle \overline{p_f} \rangle = 2\frac{(\log(D))^2(1+s_1)}{D^{1+s_1}-1}\langle s_{eff} \rangle$, where the average $\langle \rangle$ is taken over all L possible double mutants, and for brevity we have used $\langle s_{eff} \rangle$ to represent $\langle \max(0, s_{eff}) \rangle$.

The average probability that a division event gives rise to a successful double mutant is therefore $\mu\langle\overline{p_f}\rangle$, and P_{u1}, being the probability that none of these division events give rise to a successful double mutant, is given by

$$
\begin{aligned}
P_{u1} &= e^{-\mu\langle\overline{p_f}\rangle(D^{1+s_1}-1)} \\
&= e^{-\tilde{\mu}\langle\tilde{s}_{eff}\rangle}
\end{aligned}
\tag{S14}
$$

where $\tilde{s}_{eff} = \log(D)s_{eff}$ and $\tilde{\mu} \approx 2\mu\log(D)$ for $|s_1| \ll 1$.

Substituting this expression for P_{u1} into Eqn. S12 and defining $\tilde{s}_1 = \log(D)s_1$, the probability $p_d = 1 - P_{uext}$ of a successful double mutant occurring from a single mutant at the start of a day satisfies the equation:

$$
\log(1 - p_d) = -\tilde{\mu}\langle\tilde{s}_{eff}\rangle - e^{\tilde{s}_1}p_d
\tag{S15}
$$

Taking the limit $p_d \ll 1$,

$$
\begin{aligned}
p_d &= \tilde{s}_1 + \sqrt{\tilde{s}_1{}^2 + 2\tilde{\mu}\langle\tilde{s}_{eff}\rangle} \\
&= \begin{cases} \sqrt{2\tilde{\mu}\langle\tilde{s}_{eff}\rangle}, \text{ for } \tilde{s}_1{}^2 \ll 2\tilde{\mu}\langle\tilde{s}_{eff}\rangle \ll 1 \\ -\frac{\tilde{\mu}\langle\tilde{s}_{eff}\rangle}{\tilde{s}_1}, \text{ for } 2\tilde{\mu}\langle\tilde{s}_{eff}\rangle \ll \tilde{s}_1{}^2 \ll 1 \end{cases}
\end{aligned}
\tag{S16}
$$

These expressions for p_d are the same as that for the Moran process (Eqn.4) and other related models such as the Wright-Fisher model (*12*), except for slight differences in the constant prefactors. In all of our derivations, we have assumed that deleterious mutations do not fix on their own. This assumption is valid if the probability of a neutral mutation fixing is much less than the probability of it gaining a successful second mutation i.e. $N_0 \gg 1/\sqrt{2\tilde{\mu}\langle\tilde{s}_{eff}\rangle}$.

Just like in the derivation of $p_f(s, \tilde{t})$ for a single mutant (Eqn. S11), here it is also possible to take into account the time at which the first mutant occurs. Following the same derivation as above, the average probability of a successful double mutant occurring from a single mutant that emerges at $\tilde{t}_1$ is then given by

$$
p_d(\tilde{t}_1) \approx D^{-\tilde{t}_1} p_d(\tilde{t}_1 = 0)
\tag{S17}
$$

and averaging over all possible t_1, with $P(\tilde{t}_1)$ again given by Eqn.S9, the average probability of

a successful second mutation given that a single mutant of s_1 has emerged is found to be

$$
\begin{aligned}
\overline{p_d} &= \int_0^1 p_d(\tilde{t}_1)P(\tilde{t}_1)d\tilde{t}_1 \\
&= \frac{\log(D)}{D-1}p_d(\tilde{t}_1 = 0)
\end{aligned}
\tag{S18}
$$